

Involvement of NF- κ B/miR-448 regulatory feedback loop in chemotherapy-induced epithelial–mesenchymal transition of breast cancer cells

Q-Q Li¹, Z-Q Chen², X-X Cao¹, J-D Xu¹, J-W Xu¹, Y-Y Chen¹, W-J Wang², Q Chen¹, F Tang², X-P Liu^{*1} and Z-D Xu^{*2}

The epithelial–mesenchymal transition (EMT) induced by chemotherapeutic agents promotes malignant tumor progression; however, the mechanism underlying the drug-induced EMT remains unclear. In this study, we reported that miR-448 is the most downregulated microRNA following chemotherapy. Suppression of miR-448 correlated with EMT induction in breast cancer *in vitro* and *in vivo*. With the use of chromatin immunoprecipitation-seq analysis, we demonstrated that miR-448 suppression induces EMT by directly targeting special AT-rich sequence-binding protein-1 (SATB1) mRNA, leading to elevated levels of amphiregulin and thereby, increasing epidermal growth factor receptor (EGFR)-mediated Twist1 expression, as well as nuclear factor κ B (NF- κ B) activation. On the other hand, we also found that the adriamycin-activated NF- κ B directly binds the promoter of miR-448 suppressing its transcription, suggesting a positive feedback loop between NF- κ B and miR-448. Furthermore, all patients who received cyclophosphamide (CP), epirubicin plus taxotere/CP, epirubicin plus 5-fluorouracil chemotherapy showed miR-448 suppression, an increased SATB1, Twist1 expression and acquisition of mesenchymal phenotypes. These findings reveal an underlying regulatory pathway, in which the autoregulation between NF- κ B and miR-448 is important for restrain miR-448 suppression upon chemotherapy and may have a role in the regulation of chemotherapy-induced EMT. Disruption of the NF- κ B–miR-448 feedback loop during clinical treatment may improve the chemotherapy response of human breast cancers in which EMT is a critical component.

Cell Death and Differentiation (2011) 18, 16–25; doi:10.1038/cdd.2010.103; published online 27 August 2010

Chemotherapy is a systemic treatment that destroys reproducing cells, but it cannot differentiate between normal and cancerous cells. Side effects occur when normal cells become damaged. Apart from the side effects of cancer chemotherapy, unexpected ‘opposite effects’ of chemotherapy, which enhance the critical steps in malignancy rather than inhibiting them,^{1–3} have attracted progressively more attention, suggesting that novel strategies should be developed to reverse these opposite effects and render chemotherapy more effective.

Tumor cells progress from non-invasive to malignant phenotypes via a series of critical steps that involve morphological changes referred to as the epithelial–mesenchymal transition (EMT).⁴ EMT is a process originally observed during the embryonic development, in which cells lose epithelial characteristics.^{5–10} With respect to the chemotherapy, recent studies have demonstrated a close link between EMT and insensitivity to chemotherapeutic agents. Hiscox *et al.*¹¹ showed increased β -catenin expression and elevated levels of transcription of β -catenin target genes known to be involved in tumor progression and EMT in the tamoxifen

(TAM)-resistant MCF7 cells. Kajiyama *et al.*¹² identified an association between chronic paclitaxel resistance and induction of EMT in epithelial ovarian carcinomas. In addition, we previously showed that transient adriamycin treatment-induced EMT and apoptosis simultaneously in a cell-cycle-dependent manner in breast cancer cells. Only the cells undergoing EMT showed enhanced invasion/metastasis and multidrug resistance.¹³ Thus, EMT contributes to the malignant phenotypes of epithelial cancers in response to chemotherapy. Despite of these observations, however, an understanding of the precise molecular mechanisms mediating chemotherapy-induced EMT is still developing.

As EMT has a central role in cancer metastasis, it is not surprising that a staggering number of regulators are associated with this fundamental process. Recently, microRNAs (miRNAs) have appeared as powerful master regulators of EMT. miRNAs are small 20 to 22 nucleotide noncoding RNAs that inhibit gene expression at the post-transcriptional level.¹⁴ Each of the miRNAs, known to exist in mammalian cells, have multiple targets, making them

¹Department of Pathology, Shanghai Medical College, Fudan University, Shanghai 200032, China and ²Department of Pathology, Huashan Hospital, Fudan University, Shanghai 200040, China

*Corresponding author: X-P Liu or Z-D Xu, Department of Pathology, Shanghai Medical College, Fudan University, no.138 Yi Xue Yuan Road, Shanghai 200032, China. X-P Liu, Tel: +86 21 54237536; Fax: +86 21 54237596; E-mail: xpliu1228@fudan.edu.cn or Z-D Xu, Tel: +86 21 54237528; Fax: +86 21 54237596; E-mail: zdxu@shmu.edu.cn

Keywords: miR-448; chemotherapy; EMT; SATB1; amphiregulin-EGFR; NF- κ B

Abbreviations: EMT, epithelial–mesenchymal transition; miRNA, microRNA; TSS, transcription start site; ChIP, chromatin immunoprecipitation; SATB1, special AT-rich sequence-binding protein-1; AR, amphiregulin; EGFR, epidermal growth factor receptor; NF- κ B, nuclear factor κ B; CK, cytokeratin; DM, daunomycin; CP, cyclophosphamide; 5-FU, 5-fluorouracil; TAM, tamoxifen; CEF, cyclophosphamide, epirubicin plus 5-fluorouracil; CET, cyclophosphamide, epirubicin plus taxotere; CMF, cyclophosphamide, methotrexate plus 5-fluorouracil; MAPK, mitogen-activated protein kinase

Received 06.1.10; revised 21.7.10; accepted 22.7.10; Edited by M Oren; published online 27.8.10

powerful regulators of complex processes, such as differentiation and cancer progression.^{14–21} Emerging findings suggest that miRNAs contribute to the process of EMT. For example, miR-21 has pro-oncogenic effects as a result of its ability to inhibit several tumor and metastasis suppressors,²² whereas miR-200 acts as an EMT suppressor via inhibition of ZEB1 and ZEB2.^{23–28}

In this study, we report the discovery of miR-448, the most downregulated miRNA in chemotherapy-treated breast cancer cells, as direct transcriptional target of nuclear factor κ B (NF- κ B). miR-448 suppression directly promoted special AT-rich sequence-binding protein-1 (SATB1) expression, which initiates amphiregulin (AR)–epidermal growth factor receptor (EGFR) signaling toward Twist1 expression and NF- κ B activation via mitogen-activated protein kinase (MAPK) and PI3K/Akt pathway, respectively, providing a distinct positive feedback mechanism leading to EMT. These findings reveal a regulatory feedback loop to retain miR-448 suppression upon chemotherapy and suggest that the loss of miR-448 may represent a novel mechanism leading to EMT in human breast cancer.

Results

miR-448 is significantly downregulated during the course of chemotherapy-induced EMT.

After 36 h of culturing MCF7 cells with adriamycin (25 μ g/ml), analysis of array hybridization revealed 113 differentially expressed miRNAs (Supplementary Table S1). miR-448 was further investigated because it was the most significantly changed miRNA in the drug-treated cells (Figure 1a, Supplementary Table S1). miR-448 was confirmed by qRT-PCR to be markedly downregulated (Figure 1b). We used miR-126 as a control miRNA and RUN6B as a normalization control, both of which were uniformly expressed in MCF7 cells treated with or without adriamycin. After MCF7 cells were cultured with different amounts of adriamycin for 36 h, a clear dose-dependent effect of adriamycin on miR-448 suppression was observed, consistent with decreased expression of E-cadherin and upregulation of vimentin in a dose-responsive manner (Figure 1c). This correlation suggests that miR-448 suppression might have a causal role in the chemotherapy-induced EMT.

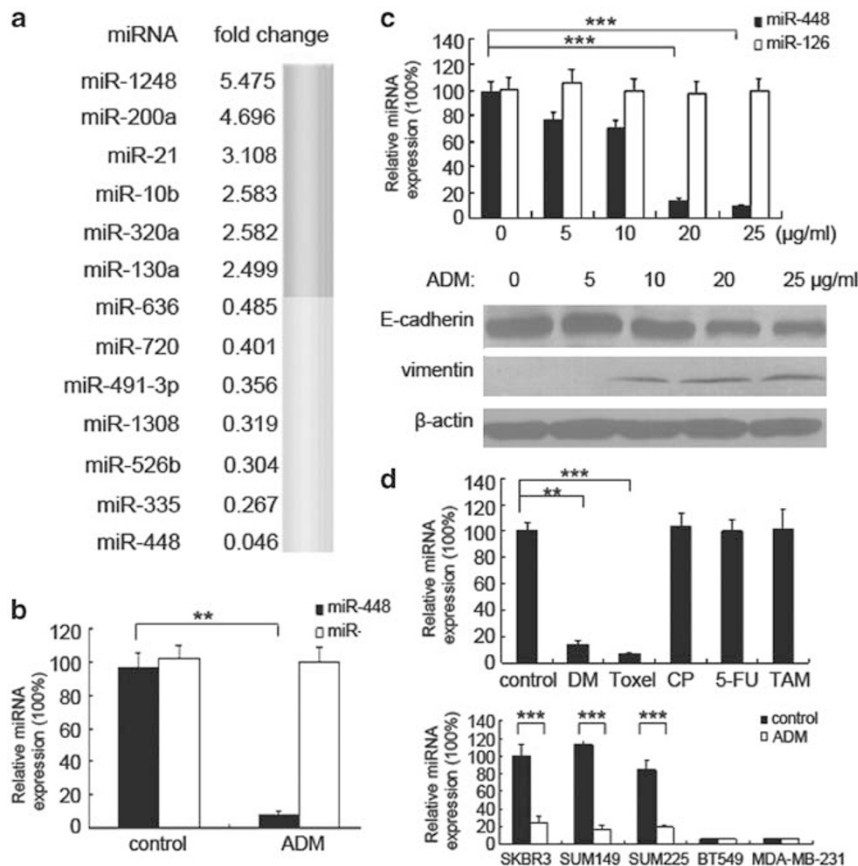


Figure 1 Dysregulation of miRNA and miR-448-mediated induction of EMT in human breast cancer cells on chemotherapy. (a) A list of significantly decreased or increased (fold change > 1.5) miRNAs in adriamycin-treated MCF7 cells. (b) After MCF7 cells were incubated with adriamycin (peak plasma concentration (PPC) 0.6 μ g/ml) for 72 h, miR-448 suppression was confirmed by qRT-PCR analysis. The data were normalized to the level of RUN6B mRNA in each sample. (c) MCF7 cells were treated with different amounts of adriamycin for 36 h after which miR-448 qRT-PCR and immunoblotting of E-cadherin and vimentin were performed. (d) MCF7 cells were cultured with or without daunomycin (DM, PPC 0.41 μ g/ml), paclitaxel (toxol, PPC 6.8 μ g/ml), CP (PPC 6 μ g/ml), 5-FU (PPC 50 μ g/ml) or TAM (PPC 40 ng/ml) for 72 h, and subjected to miR-448 qRT-PCR. miR-448 levels were normalized to the control. Alternatively, SKBR3, SUM149, SUM225, BT549 and MDA-MB-231 cells were cultured with or without adriamycin and subjected to miR-448 qRT-PCR. miR-448 levels were normalized to SKBR3 control cells. Columns, mean ($n = 3$); bars, S.D. ** $P < 0.05$, *** $P < 0.001$ by t -test

Apart from adriamycin, similar 7- and 14-fold suppression of miR-448 were also achieved by antitumor antibiotics (daunomycin (DM)) and plant alkaloids (paclitaxel), respectively. This was in contrast to exposure to alkylating agents (cyclophosphamide (CP)), anti-metabolism agents (5-FU) and non-steroid antiestrogen (TAM), which did not change miR-448 levels (Figure 1d). We then investigated miR-448 levels in a series of human breast carcinoma cell lines. Endogenous miR-448 levels were significantly higher in epithelial breast cancer cells (SKBR3, SUM149 and SUM225) than in cells constitutively exhibiting mesenchymal phenotypes (BT-549 and MDA-MB-231). Moreover, miR-448 suppression on adriamycin treatment was only specific to epithelial cancer cells, whereas its levels remained unchanged in mesenchymal cancer cells treated with or without adriamycin (Figure 1d).

miR-448 negatively regulates drug-induced EMT. We next transfected the miR-448 inhibitors into MCF7 cells to determine the role of miR-448 in the drug-induced EMT. As shown in Figure 2A, the miR-448 inhibitor-induced EMT in MCF7 cells, characterized by acquisition of a fibroblast-like cell morphology, dissolution of tight junctions (ZO-1), formation of actin stress fibers (F-actin), severe E-cadherin suppression and enhanced vimentin expression (Figure 2B), similar to the effects observed in the drug-treated cells. Meanwhile, cell migration and Matrigel invasion rates were increased 5.5- and 6.5-fold, respectively, upon miR-448 downregulation (Figure 2C), without any change in cell proliferation (Supplementary Figure S1). On the contrary, when we introduced the miR-448 precursor into MDA-MB-231 cells, which express miR-448 at a negligible level and typically have a mesenchymal phenotype,

mesenchymal–epithelial transition was induced (Figure 2A and B), accompanied with a more than threefold decrease in cell migration and invasiveness (Figure 2C), without affecting the viability of these cells (Supplementary Figure S2).

Similar effects were observed *in vivo*. The control MCF7 tumors were strictly non-invasive, as shown by their confinement within fibrotic capsules (Figure 2D, a). In stark contrast, 7 out of 10 miR-448-silenced tumors showed a spindle-like morphology, with islands of cancer cells that had invaded the muscle (Figure 2D, b). Immunohistochemical analyses further confirmed that the miR-448-silenced tumor cells were positive for both epithelial and mesenchymal markers (Figure 2D, d and f), whereas the control tumors showed positive only for epithelial markers (Figure 2D, c and e). At 6 weeks after implantation, the lungs of mice implanted with miR-448-silenced cells exhibited small clusters of heteromorphic cells that were positive for either CK19 or vimentin (Figure 2D, h, j, l). In the lungs of hosts bearing control MCF7 tumors, however, no metastatic foci were found and the only CK19-positive cells were normal bronchial epithelial cells (Figure 2D, g, i, k).

Non-aggressive tumors arose in 3 of 10 miR-448-inhibitor-treated MCF7 tumors, which was a result of plasmid loss rather than biological resistance to miR-448-mediated EMT, as determined by quantifying miR-448 expression by qRT-PCR (Supplementary Figure S3).

NF- κ B directly transsuppresses miR-448 in parallel with its host gene, *HRT2C*. We then investigated the potential transcription factors involved in the upstream regulation of miR-448. miR-448 has been mapped to the fourth intron of *HRT2C* on chromosome X (Supplementary Figure S4A). An algorithmic prediction of potential transfactor binding sites

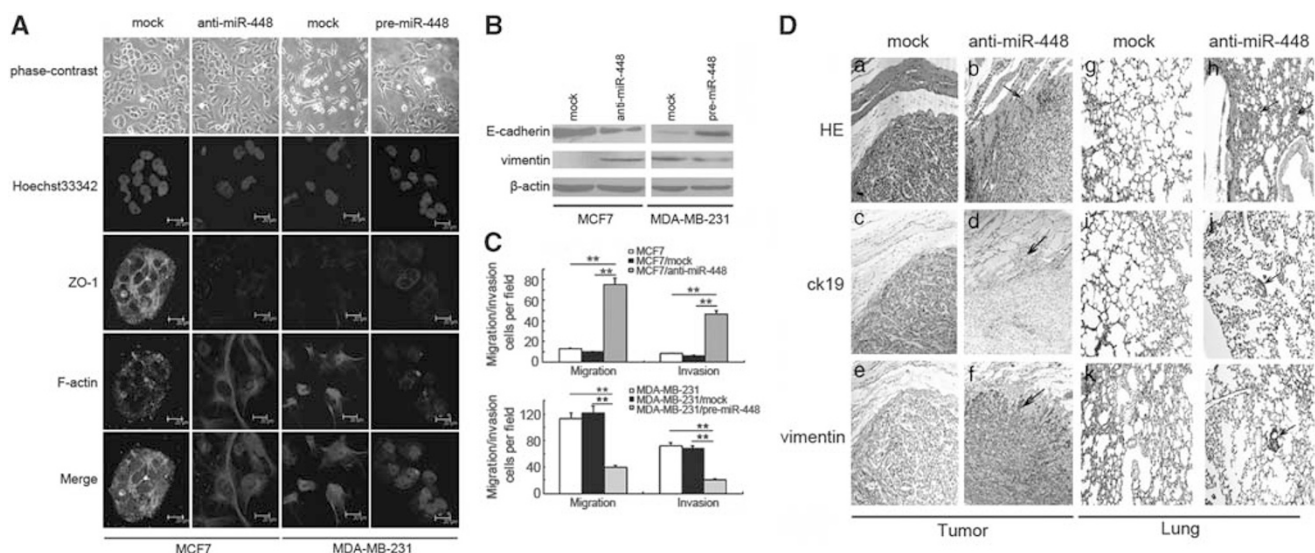


Figure 2 miR-448 suppression induces EMT and tumor metastasis. MCF7 and MDA-MB-231 cells were transfected with anti-miR-448 inhibitor or pre-miR-448 respectively. (A) EMT was examined by phase-contrast photomicrographs and by immunofluorescent staining for ZO-1 (green), F-actin (red) and nuclei (blue, Hoechst33342). (B) E-cadherin and vimentin expression levels were detected by immunoblotting. (C) The transwell migration/invasion assays were performed at 36 h after transfection. (D) (a, b, g, h) Hematoxylin and eosin (HE)-, (c, d, i, j) CK19- and (e, f, k, l) vimentin-stained sections of primary tumors and lungs isolated at week 9 after transplantation from mice receiving orthotopic injection of anti-miR-448-transduced or mock-infected MCF7 cells. Arrows in panels indicate areas of muscular invasion and clusters of metastatic cells in lungs. Columns, mean ($n=3$); bars, S.D. ** $P < 0.05$ by *t*-test. Scale bars: (A, D) 10 μ m

was performed using MatInspector software (Genomatix Software GmbH, Munich, Germany). Putative-binding sites for NF- κ B, AP1, c-Myc and AP4 were identified (Supplementary Figure S4B). The miR-448 promoter activity was evaluated after cotransfection of these candidate transactors. Expression of NF- κ B was associated with a significant decrease in miR-448 promoter activity, whereas AP1, c-Myc and AP1 had no effect on promoter activity (Supplementary Figure S4C), suggesting that miR-448 may be a downstream factor of NF- κ B.

Previous studies involving the genome-scale analysis of transcription factor binding predicts that a significant fraction of miRNAs appear to be located within the introns of protein-encoding genes, linking their expression to the promoter-driven regulation of their host genes. In agreement with this prediction, qRT-PCR assays showed that *HRT2C* expression was also downregulated by NF- κ B activation on adriamycin treatment, to a similar extent as miR-448. We next evaluated NF- κ B binding activity in adriamycin-treated cells by EMSA. NF- κ B activity was induced at 6 h after treatment, earlier than

HRT2C/miR-448 suppression (Figure 3a). Similar effects were also observed in MCF7 and SUM149 cells treated with PMA, a specific activator of NF- κ B (Figure 3b).

To further confirm the binding of NF- κ B to the promoter of *HRT2C*/miR-448, we performed chromatin immunoprecipitation (ChIP)-qPCR experiments in adriamycin, DM or PMA-treated MCF7 cells using the NF- κ B antibody. To this end, we used a series of PCR primers covering genomic regions surrounding the transcription start site (TSS), and the results detected a strong PCR amplification in the core promoter region corresponding to the predicted NF- κ B-binding site, but not in the surrounding region up/downstream of miR-448. Similar effects were also observed in SUM149 cells on adriamycin, DM or PMA treatment (Figure 3c). Furthermore, to validate the regulation of NF- κ B on miR-448 expression, cultured MCF7 or SUM149 cells were pretreated by NF- κ B p65 siRNA, and then stimulated by adriamycin for another 72 h. Adriamycin-induced downregulation of miR-448 was significantly suppressed by NF- κ B p65 siRNA in both MCF7 and SUM149 cells. (Figure 3d). Thus, these results support

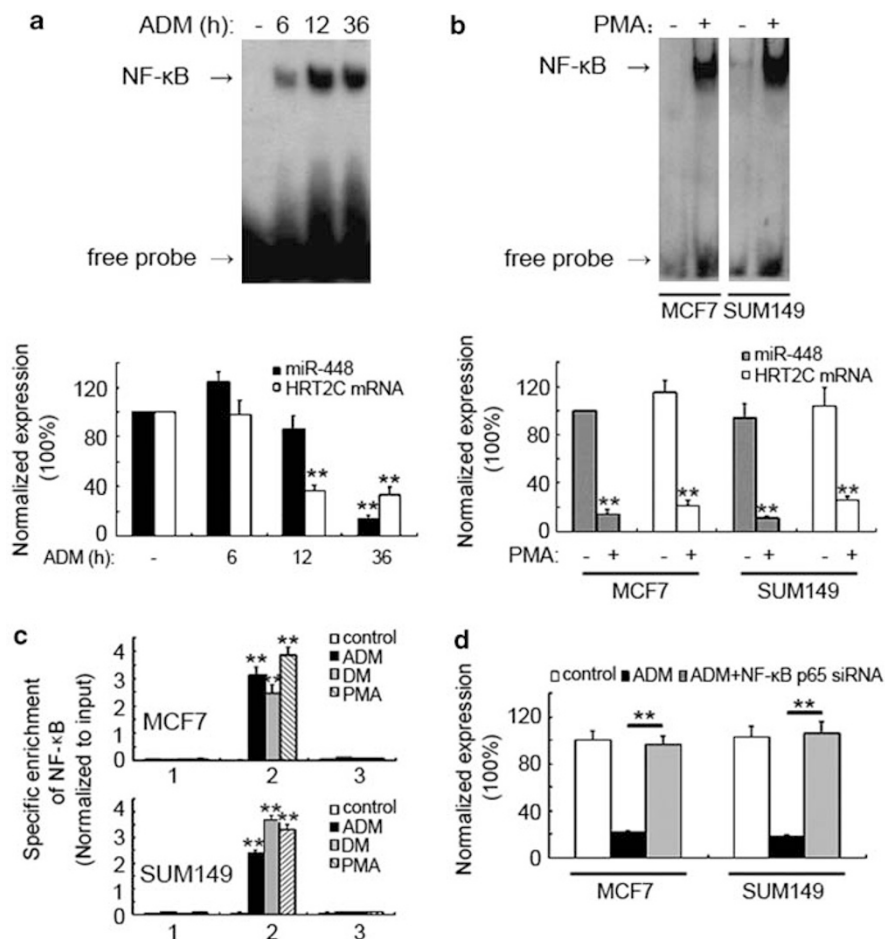


Figure 3 Direct transcriptional suppression of miR-448 by NF- κ B. qRT-PCR of miR-448, *HRT2C* and activity of NF- κ B were performed in MCF7 cells following adriamycin (a) or PMA (b) treatment for indicated times. (c) MCF7 and SUM149 cells were treated with or without adriamycin or PMA for 24 h before ChIP analysis using NF- κ B antibody. Genomic DNA fragments covering region surrounding the miR-448 TSS as indicated in a were analyzed by real-time PCR. Enrichment was normalized to input control. (d) After pre-treating with NF- κ B p65 siRNA, miR-448 expression levels in adriamycin-treated MCF7 and SUM149 cells were determined by real-time PCR. Columns, mean ($n=3$); bars, S.D. ** $P<0.05$ by *t*-test

the notion that *HRT2C* and hosted miR-448 share a common negative regulatory element located within the fourth intron of *HRT2C* gene, and that the transcriptional unit is transcriptionally suppressed by NF- κ B.

miR-448 suppression directly targets and promotes SATB1 expression. Among the approximately 100 targets predicted by the TargetScan32 and PicTar33 search programs, SATB1 was of particular interest, given that it is an important piece of the cascade that initiates EMT and promotes tumor metastasis. SATB1 has two potential miR-448-binding sites within its 3'-UTR, which are highly conserved in various analyzed species (Figure 4a). Reporter plasmids were constructed, in which portions of the 3'-UTR encompassing the predicted binding sites (SATB1wt), with or without mutations that would disrupt miRNA interaction (SATB1mut1 and SATB1mut2), were cloned downstream of a luciferase open reading frame. When introduced into MCF7 cells, the SATB1wt and SATB1mut1 constructs were expressed at significantly lower levels than the SATB1mut2 and SATB1v constructs, consistent with the direct functional interaction of endogenously expressed miR-448 with binding site 2. Cotransfection of reporter plasmids with a synthetic miR-448 inhibitor or miR-448 precursor further restored or abolished the luciferase activity produced by the wild-type and mut1 reporter constructs, but had no effect on mut2 reporter constructs (Figure 4b).

When MCF7 cells were cultured in adriamycin-containing medium for 72 h, adriamycin-induced SATB1 expression at both mRNA and protein levels, which were largely abrogated by ectopic miR-448 expression (Figure 4c). Importantly, antisense inhibition of miR-448 resulted in a moderate but significant increase in the level of endogenous SATB1 in MCF7 cells (Figure 4d), and this effect was abolished by cotransfection with pre-miR-448 and/or a siRNA directed against SATB1 (Figure 4d). In parallel, pre-miR-448 treatment

in MDA-MB-231 cells, which express miR-448 negligibly, resulted in decreased expression of SATB1 (Figure 4d). Both down- and upregulation of miR-448 appear to be physiologically relevant, given that they affected the levels of SATB1 within the physiologically relevant range observed in the epithelial *versus* the mesenchymal phenotype.

miR-448-mediated SATB1 expression correlates with activation of AR-EGFR pathway. To identify the direct targeted genes of SATB1 in response to adriamycin treatment, we performed ChIP-seq of the DNAs from anti-SATB1 chromatin IP. A histogram of SATB1-binding sites residing within the downstream 2 kb or upstream 3 kb genomic regions relative to annotated TSSs is shown in Supplementary Figure S5A. Most of the SATB1-binding regions were identified around the TSS sites. The consensus sequence derived from the most frequent motifs found in the SATB1-bound promoters corresponds to a perfect SATB1 response element TATTAGTAATAA (Supplementary Figure S5B). Using a false discovery rate cutoff of 0.05, we identified a total of 538 SATB1-binding regions in the adriamycin-treated MCF7 cells (Supplementary Table S2). These results were further intensely analyzed by Gene Ontology. According to the biology function classification, 38 of 538 genes were associated with transcription, 37 were related to transport and 23 were involved in signal transduction (Supplementary Figure S5C). The mostly strong SATB1-binding region by the number of sequence tags mapped is the gene for AR (Supplementary Figure S5D, Supplementary Table S2). With an antibody against SATB1, substantial enrichment of the region spanning the AR was observed in the adriamycin-treated MCF7 and SUM149 cells, similar to what was observed after 72 h of treatment with DM or paclitaxel. In a luciferase reporter assay, the pGL3-AR promoter is induced by the expression of SATB1 by approximately eightfold. Treatment with adriamycin further

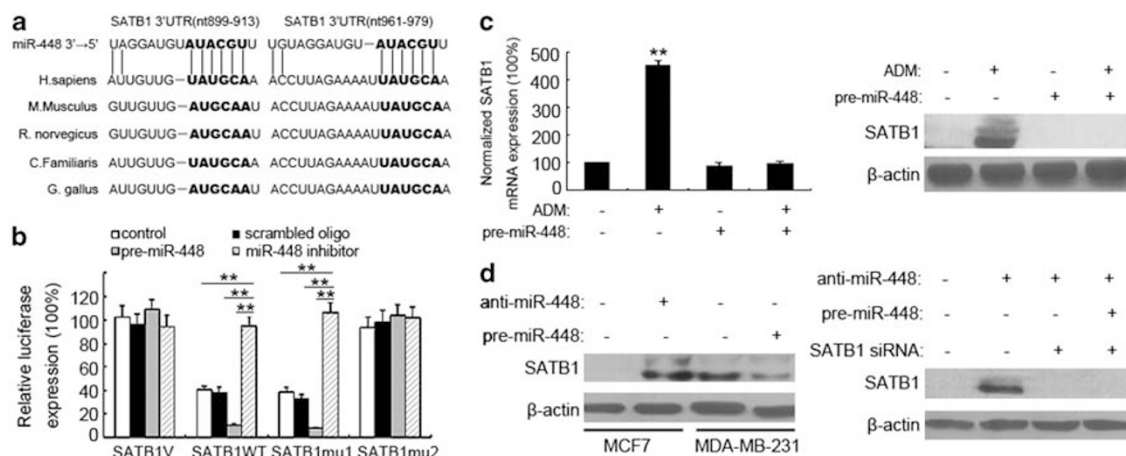


Figure 4 Chemotherapy-induced miR-448 suppression directly targets and promotes SATB1 expression. (a) Alignment of potential miR-448-binding sites in the 3'-UTR of the SATB1 mRNA of different species. (b) Reporter vectors lacking 3'-UTR (SATB1V) or containing the 3'-UTR of the wild-type SATB1 mRNA (SATB1WT) or a 3'-UTR with mutated miR-448-binding sites (SATB1 mut1 and SATB1 mut2) were cotransfected along with miR-448 inhibitors or precursors into MCF7 cells, after which the luciferase activity was measured using the dual-luciferase reporter assay system. (c) qRT-PCR and Immunoblotting for SATB1 in pre-miR-448- infected MCF7 cells treated with or without adriamycin. (d) The expression levels of SATB1 in anti/pre-miR-448-infected MCF7 and MDA-MB-231 cells were determined by immunoblotting. Immunoblotting of SATB1 was also performed in anti-miR-448-transfected MCF7 cells upon SATB1 siRNA or pre-miR-448 treatment. Columns, mean ($n = 3$); bars, S.D. $**P < 0.05$ by *t*-test

enhanced secretion of AR in a dose-dependent manner, which was blocked by SATB1 siRNA (Figure 5a). These results recapitulate the native expression pattern of the gene in MCF7 cells and verify a SATB1-dependent activation mechanism.

AR has been shown to possess EGF-like activity. Treatment with miR-448 inhibitors led to both upregulation and phosphorylation of EGFR in MCF7 cells, following by subsequent activation of MAPK and Akt, but not STAT3 in downstream of the signaling pathway. These effects were largely abrogated by cotransfection with a siRNA directed against SATB1 or AR, suggesting the involvement of SATB1–AR–EGFR axis in this process (Figure 5b). On one hand, inhibition of MAPK disrupted the adriamycin-induced Twist expression, a master regulator of EMT (Figure 5c). On the other hand, a specific Akt inhibitor (LY294002) significantly suppressed adriamycin-induced I κ B α degradation and NF- κ B activity. Thus, our data indicate that NF- κ B-mediated miR-448 suppression promotes the expression of SATB1, which enhances NF- κ B activity and increases Twist1 expression by initiating AR–EGFR pathway, thereby providing a positive feedback loop mechanism to restrain miR-448 suppression and lead to EMT (Figure 5d).

miR-448 suppression correlates with SATB1 expression and the acquisition of mesenchymal phenotypes in post-chemotherapy human breast carcinoma. To establish the clinical relevance of miR-448 regulation in chemotherapy-induced effects, we assessed miR-448 expression and tumor phenotypes in 18 patients with breast carcinoma who had paired tumor specimens available from before and after chemotherapy. Representative sections showing SATB1, Twist1, CK19 and vimentin staining are shown in Figure 6, and results for individual patients are listed in Table 1 and Supplementary Table S3.

Although the morphology of breast carcinomas after chemotherapy did not differ markedly from native tumors, the six patients who received the CP, epirubicin plus taxotere (CET) or CP, epirubicin plus 5-fluorouracil (5-FU) regimen showed a reduction in miR-448 expression ($P=0.02$, paired t -test), whereas the patients who received the CP, methotrexate plus 5-FU (CMF) regimen showed the stable levels of miR-448 (Table 1). Moreover, control miR-126 showed no difference in the expression level in all cases (data not shown). Immunohistochemical staining revealed focally positivity of the tumor cells for both SATB1 and Twist1 in 12 patients who received the CET/CEF regimen. These phenomena correlated with partial loss of the epithelial marker CK19 and acquisition of vimentin expression (Figure 6 and Supplementary Table S3), illustrating that the phenotypic changes paralleled miR-448 suppression. Similar results were not detected, however, in the patients who received the CMF regimen (Supplementary and Supplementary Table S3).

Discussion

Many patients with cancers experience a relapse after treatment with the currently available adjuvant chemotherapies, primarily because of the residue tumor cells. Although

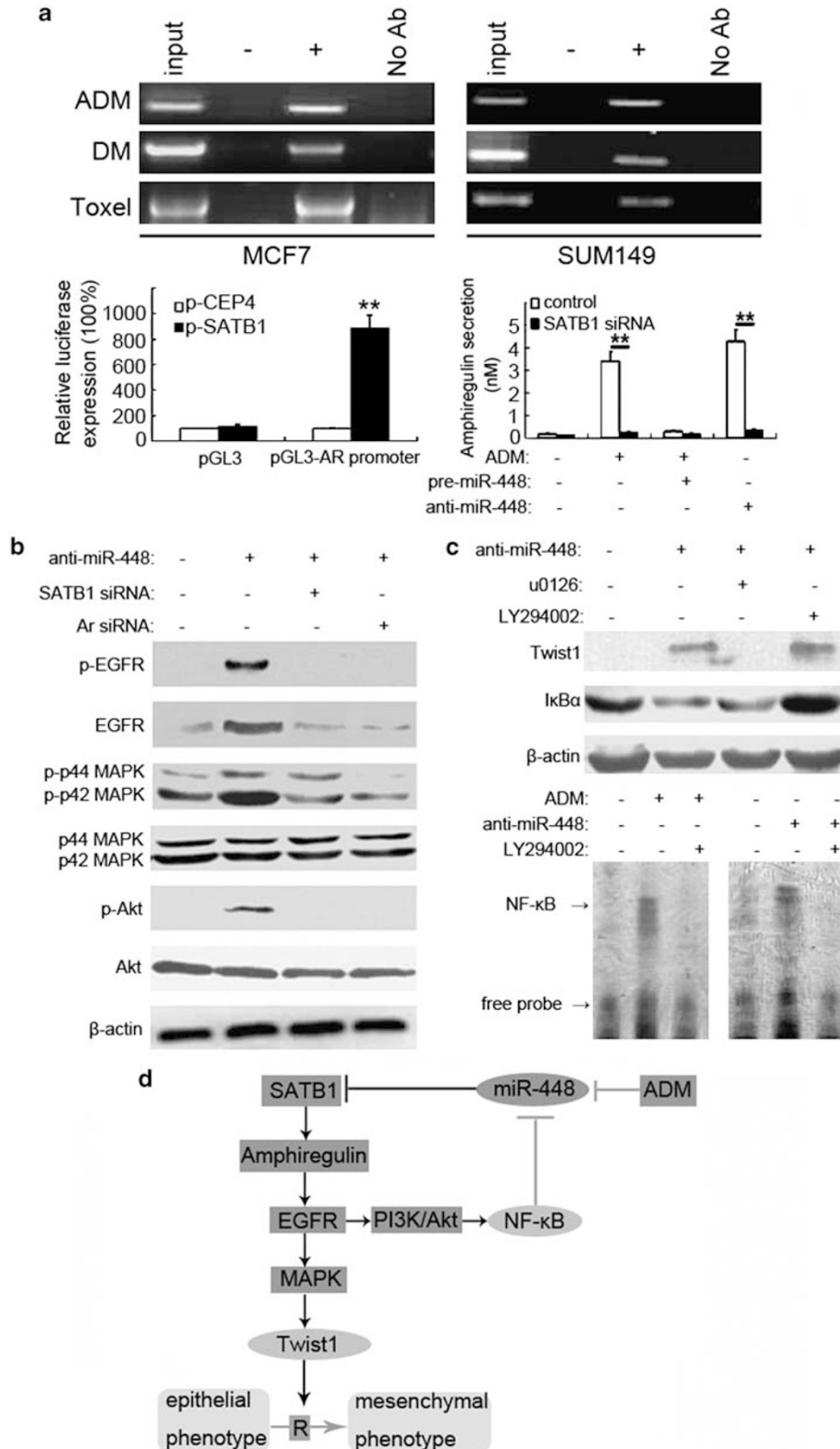
some cells in a tumor are killed by chemotherapy agents (apoptosis), the surviving cells undergo EMT which promotes not only cell survival but also cell metastasis and resistance to chemotherapy.¹³ This highlights the strong need for rational, mechanism-based therapies. One approach with great potential to achieve this goal is the identification and targeting of key substances involved in EMT.

Our findings are of importance to the understanding of chemotherapy-induced EMT in breast tumors, as they directly link miR-448 to this process. Chemotherapy-induced miR-448 suppression enables the MCF7 cells to acquire mesenchymal characteristics associated with invasive and metastatic behavior *in vitro* and *in vivo*. Further, silencing of miR-448 exerts the pro-EMT effects by directly targeting and promoting SATB1 expression. SATB1, a genome organizer, is an important step in the cascade that initiates EMT and metastasis in breast tumors. It reprogrammes chromatin organization and the transcription profiles of breast tumors to act as a determinant of morphogenesis and metastasis.²⁹ Herein, an inverse correlation was found between miR-448 and SATB1 in drug-treated breast cancer cell lines, in post-chemotherapy human breast samples, and in tumor-implanted mice. We proposed that miR-448 suppression is pivotal in the process of chemotherapy-induced EMT. Several studies comparing the miRNA expression profiles between epithelial and mesenchymal tumor cells have established the functional role of miRNAs in EMT. It is likely that other endogenous miRNAs, such as miR-200,^{23–27} miR-205^{24,30} and miR-21,^{22,31} also have related pro- or anti-EMT functions and that miR-448 may belong to a family of miRNAs involved in EMT. We have detected several members of the miR-200 family, as well as miR-21 and miR-10b, in MCF7 cells. Under the conditions of used in our study, these miRNAs appeared to be down- or upregulated in MCF7 cells exposed to adriamycin. Thus, although various miRNAs have been implicated in chemotherapy-induced EMT in epithelial breast cancers, miR-448 has a dominant and functional role in this process.

It is interesting to note that miR-448 has a significant regulatory effect on SATB1 expression in epithelial/mesenchymal breast cancer cells, although additional factors (including other miRNAs) cannot be absolutely excluded. It has been proved that knockdown of SATB1 in highly aggressive cancer cells results in altered expression of more than 1000 genes, many of which are known to be involved in oncogenic pathways.²⁹ In this study, we have undertaken a global screening approach to identify the promoters that are bound by SATB1 under chemotherapy. AR, the EGFR ligand, showed a distinct SATB1-dependent expression in adriamycin-treated MCF7 cells. Initially, the goal of the ChIP-seq screen was to determine the promoter specificity of SATB1 during adriamycin treatment, but our subsequent analysis revealed that SATB1 bound the same targets regardless of the drugs used, suggesting the common mechanism of transcriptional regulation by SATB1. AR has been shown previously to induce differential effects through the EGFR signaling, contributing to the progression of several cancers.^{32–35} The literature showing a connection between AR and EMT is not extensive. A link between EGFR and EMT was found previously; however, these studies have implied that EMT may contribute to resistance to EGFR-directed

therapy.^{36–38} As demonstrated in this study, an inhibitor of EGFR/MAPK signaling reduced Twist1 expression, a master regulator of EMT, in the adriamycin-treated cells; nevertheless, it exerted no effects on adriamycin-induced NF- κ B

activation, which was later shown to be because of the PI3K/Akt pathway. Hence, our studies are the first to identify Twist1, as well as NF- κ B, downstream of the EGFR on adriamycin treatment, suggesting a possible connection between



of them in the context of SATB1-mediated AR expression.

Furthermore, NF- κ B is indeed recruited to the miR-448/HRT2C promoter region to suppress miR-448 expression in adriamycin-treated MCF7 cells, demonstrating the existence

of a functional NF- κ B-regulated suppressor upstream of the *miR-448/HRT2C* gene. Activation of NF- κ B has been observed after chemotherapy, which is linked to E-cadherin downregulation and Snail family induction, thereby initiates an

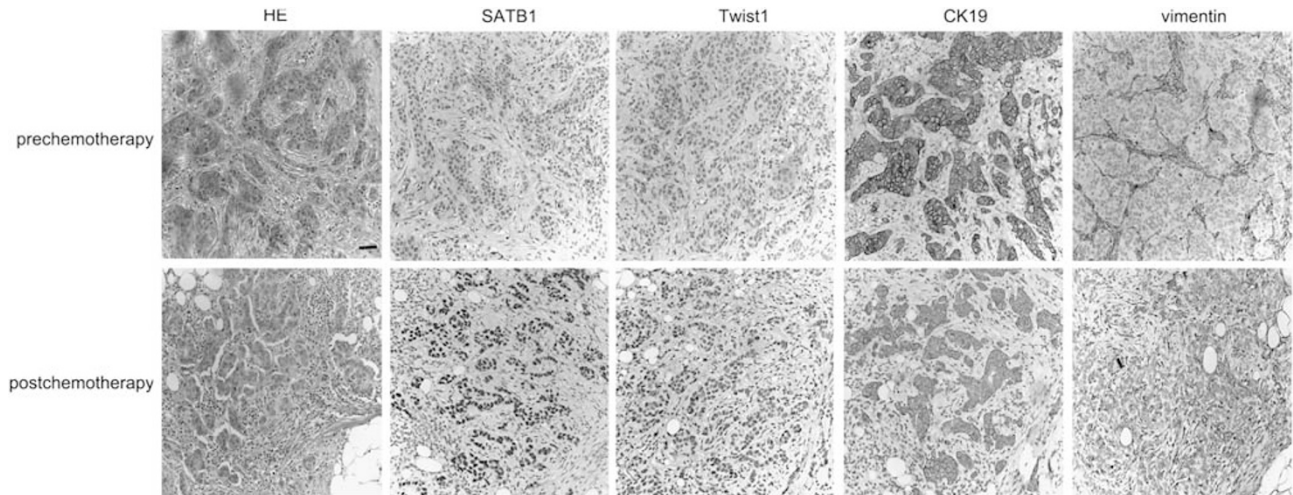


Figure 6 Immunophenotypes of tumor sections taken from breast cancer patients who received the CET/CEF regimen. Hematoxylin and eosin (HE)-, SATB1-, Twist1-, CK19- and vimentin-stained sections of primary mammary tumors taken from patient 7 before (upper panels) and after (lower panels) four cycles of the CEF regimen. Scale bars: 10 μ m

Table 1 Summary of results

Patient	WHO classification	Regimen	Delay to surgery (days)	Normalized miR-448 expression (%)	
				Before chemotherapy	After chemotherapy
1	WHO II	CET	48	100.0 (6.2)	32.7 (2.8)*
2	WHO II	CET	42	132.4 (9.1)	27.6 (1.7)*
3	WHO II	CET	53	105.3 (8.8)	30.7 (2.1)*
4	WHO III	CET	50	96.4 (7.8)	25.2 (2.3)*
5	WHO III	CET	55	113.6 (13.5)	49.2 (5.9)*
6	WHO II	CET	46	80.3 (7.7)	30.4 (3.6)*
7	WHO II	CEF	48	95.3 (8.2)	21.1 (1.8)*
8	WHO III	CEF	51	100.6 (7.9)	24.4 (5.2)*
9	WHO III	CEF	50	108.4 (9.3)	38.9 (4.5)*
10	WHO II	CEF	49	83.4 (6.2)	25.1 (3.0)*
11	WHO III	CEF	53	93.3 (9.4)	21.0 (5.6)*
12	WHO III	CEF	44	153.1 (9.0)	41.3 (4.7)*
13	WHO II	CMF	46	126.9 (10.5)	133.8 (11.4)
14	WHO II	CMF	46	94.8 (9.7)	90.3 (8.2)
15	WHO III	CMF	49	105.1 (9.6)	82.7 (7.2)
16	WHO II	CMF	55	89.3 (8.8)	90.4 (6.7)
17	WHO II	CMF	50	111.6 (10.3)	107.8 (7.1)
18	WHO II	CMF	47	82.5 (9.1)	88.6 (6.9)

Abbreviations: CEF, cyclophosphamide, epirubicin plus 5-fluorouracil; CET, cyclophosphamide, epirubicin plus taxotere; CMF, cyclophosphamide, methotrexate plus 5-fluorouracil. Normalized miR-448 expression was presented as the mean (S.E.M.) of three independent experiments. * $P < 0.05$ by paired *t*-test.

Figure 5 Identification of AR-EGFR axis as downstream pathway of SATB1. (a) Adriamycin-treated MCF7 cells were processed for ChIP using an antibody against SATB1. DNA was interrogated with primers specific for AR promoter. ‘-’ and ‘+’ represents the cells treated without or with various drugs, respectively. MCF7 cells were transfected with pCEP4/pCEP4-SATB1 and pGL3/pGL3-AR promoter, after which the luciferase activity was measured. AR ELISA on cell culture supernatants was performed in SATB1 siRNA-infected MCF7 cells treated with adriamycin, miR-448 precursor or miR-448 inhibitors. Columns, mean ($n = 3$); bars, S.D. ** $P < 0.05$ by *t*-test. (b) After MCF7 cells were transfected with anti-miR-448 inhibitor, together with or without SATB1 or AR siRNA, activation of EGFR, MAPK and Akt were evaluated by immunoblotting. (c) MCF7 cells were preincubated with or without U0126 (20 μ M) or LY294002 (20 μ M) for 1 h before stimulated with adriamycin for 72 h. Twist1 and I κ B α expression were then detected by immunoblotting. After MCF7 cells were preincubated with or without LY294002 (20 μ M) for 1 h before stimulated with adriamycin or miR-448 inhibitors for 36 h, the nuclear extracts were subjected to EMSA using a labeled NF- κ B DNA probe. (d) A proposed model of NF- κ B-miR-448 circuitry as an autoregulatory positive feedback loop in chemotherapy-induced miR-448 suppression and EMT

anti-apoptotic response and promotes mesenchymal transition in various tumors.³⁹ However, recent data suggest this regulatory route does not sufficiently explain the full pro-EMT and anti-apoptotic potential of NF- κ B. This study helps refine our understanding of NF- κ B-induced EMT, that is, miR-448 suppression by NF- κ B represents a rather slow-acting yet long-lasting stimulus, which further enhances NF- κ B activity and appears as an ideal complementation of the immediate induction of EMT. Thus, although the mechanism underlying NF- κ B activation initiated by adriamycin still remains unclear, the study herein provide a positive feedback loop mechanism to restrain miR-448 suppression, lead to EMT and resistant to drug-induced apoptosis. Integrating the use of drugs targeted to miR-448 or other key substances into specific chemotherapy regimens (anthracyclines, antitumor antibiotics or alkaloid based) might be an effective means to improve the efficacy of systemic treatment in patients with breast cancer.

Materials and Methods

Cell lines. The human mammary carcinoma cell lines, SKBR3, MCF7, MDA-MB-231 and BT549, were purchased from ATCC and were cultured under the conditions recommended by the manufacturer. SUM149 and SUM225 cell lines were a generous gift of Dr Steve Ethier (University of Michigan Medical Center).

RNA isolation and miRNA detection. Isolation of total RNA from cultured cells, with efficient recovery of small RNAs, was performed using the miRVana miRNA Isolation Kit (Ambion, Austin, TX, USA). Detection of the mature form of miR-448 was performed using the miRVana qRT-PCR miRNA Detection Kit and qRT-PCR Primer Sets, according to the manufacturer's instructions (Ambion). miR-126 was used as an internal control.

Plasmid construction and stable/transient transfection of anti-miR-448. For the transient inhibition of miR-448, 50 nM miR-448 inhibitor oligonucleotide (Ambion) were transfected into MCF7 cells using Lipofectamine 2000 (Invitrogen, Carlsbad, CA, USA) according to the manufacturer's instructions. To generate stable miR-448-depleted MCF7 transfectants, anti-miR-448 sequences were amplified from miRZip-448 construct (System Biosciences, Mountain View, CA, USA) and subcloned into pSilencer4.1 (Ambion) polyclone sites with *Hind*III and *Bam*HI sites. MCF7 cells were then transfected with the pSILENCER Expression Vector containing the antisense sequence of miR-448. Cells were selected with puromycin 48 h after transfection and then diluted to perform clonal selection.

Chromatin immunoprecipitation. MCF7 cells were exposed to adriamycin for 36 h prior to perform ChIP using antibodies against SATB1 (no. 611182, BD Bioscience) as described previously. A total of 1 to 2.5% of each IP was assayed by real-time PCR using primers specific for a region of interest. Sequencing was carried out on an Illumina 1G instrument according to the manufacturer's protocol.

In vitro migration and invasion assays. A bioassay for *in vitro* cell migration/invasion using Matrigel Invasion Chambers (Corning Costar, Corning, NY, USA) was performed as described previously.¹³

Luciferase reporter assay. Cells at 50% confluence in 24-well plates were transfected using Fugene 6 (Roche, Indianapolis, IN, USA). A firefly luciferase reporter gene construct (200 ng) and 1 ng of the pRL-SV40 Renilla luciferase construct (for normalization) were cotransfected per well. Cell extracts were prepared 48 h after transfection, and luciferase activity was measured using the Dual-Luciferase Reporter Assay System (Promega, Sunnyvale, CA, USA).

Immunoblotting. Total protein was extracted from cells using RIPA lysis buffer (Santa Cruz Biotechnology, Santa Cruz, CA, USA). Protein extract (50 μ g/lane) was electrophoresed, transferred to PVDF membranes and incubated overnight with primary antibodies against E-cadherin (sc-8426, Santa Cruz Biotechnology), vimentin (sc-32322, Santa Cruz Biotechnology), SATB1 (PRS4631, Sigma, St. Louis, MO, USA), Twist1 (AV37997, Sigma), p-EGFR (sc-101669, Santa Cruz

Biotechnology), EGFR (sc-71034, Santa Cruz Biotechnology), p-MAPK (no. 4695, Cell Signaling Technology), MAPK (no. 4370, Cell Signaling Technology, Danvers, MA, USA), p-Akt (no. 4058, Cell Signaling Technology) and Akt (no. 9272, Cell Signaling Technology), respectively. Membranes were then treated with the appropriate HRP-conjugated secondary antibodies (Invitrogen). Detection was performed using the reagents provided in the ECL + Plus kit (GE healthcare, Piscataway, NJ, USA).

Immunofluorescence confocal microscopy analysis. Confocal immunofluorescence microscopy analysis using antibodies against ZO-1 (sc-10804, Santa Cruz Biotechnology) and F-actin (ab205, Abcam, Cambridge, UK) was performed as described previously.¹³

EMSA. Protein extracts were prepared from MCF7 cells treated with adriamycin for 36 h. Protein extracts (30 μ g) was used directly for EMSA to evaluated NF- κ B activity as described previously.⁴⁰ Sequences used for EMSA are as follows (putative binding elements are underlined): 5'-AGTTGAGGGGACTTCCCAGGC-3'; 3'-TCAACTCCCCTCAAAGGGTCCG-5'.

Surgery, necropsy, histopathology and immunohistochemistry.

All animal procedures were approved by the Animal Care Committee of Fudan University. Female NOD-SCID mice (4 week old) were anesthetized with 2, 2, 2-tribromoethanol. The skin was incised, and tumor cells (2×10^6) in 0.2 ml growth medium were injected into the left flank of nude mice. A total of 10 mice per group were killed at week 9 post-transplantation. The tumors, lungs, livers, spleens and macroscopic metastases were analyzed under a dissecting microscope. Tissue samples were fixed in 10% buffered formalin for 12 h, followed by a wash with PBS and transfer to 70% ethanol, then embedded in paraffin, sectioned and stained with hematoxylin and eosin. Immunohistochemistry detection using anti-CK19 antibodies (MU246-UC, BioGenex), and anti-vimentin antibodies (MU074-UC, BioGenex, San Ramon, CA, USA) was performed on paraffin sections, using a BioGenex i6000 automated stainer.

Patient study. Patients were identified from the Huashan Hospital records. Patients were selected who had undergone a diagnostic biopsy (core or excision biopsy, not needle aspiration) or primary surgery, followed by multiple cycles of chemotherapy and then debulking surgery, provided that paraffin blocks were available for both time points. The ethics committees of the participating hospitals approved the protocol and written informed consent for the collection of tumor tissue was obtained from each patient. Sections (3 μ m) were cut from paraffin blocks onto silanized slides, and the sections were immunostained using antibodies against CK19 (MU246-UC, BioGenex), vimentin (MU074-UC, BioGenex), SATB1 (PRS4631, Sigma) and Twist1 (AV37997, Sigma) respectively. Scoring of CK19, vimentin, SATB1 and Twist1 expression were all graded from - to + + +, based on an assessment of the intensity of the reaction product, and the percentage of positive cells: score -, no reactivity or nuclear (SATB1 and Twist1)/membranous (CK19)/cytoplasmic (vimentin) reactivity in <10% of tumor cells; +, faint/barely perceptible reactivity is detected in >10% of tumor cells; + +, weak-to-moderate complete reactivity is seen in >10% of tumor cells; + + +, strong complete reactivity is seen in >10% of tumor cells. Total RNA, including small RNAs, was isolated from four 20- μ m sections from FFPE tissue blocks using the RecoverAll Total Nucleic Acid Isolation Kit (Ambion). Quantification of miR-448 by qRT-PCR was performed as previously described.

Statistical analysis. Statistics were calculated by SPSS software. The results are presented as mean \pm S.E.M. ANOVA, Student's *t*-test analysis and Dunnett's multiple comparison tests were used to compare mean values. A *P*-value of <0.05 was defined as statistical significance.

Conflict of interest

The authors declare no conflict of interest.

Acknowledgements. This work was supported by grants from the National Nature Science Foundation of China (No. 81071813 and No. 30870972). We thank members of our laboratory for helpful discussions.

1. Chaudhary PM, Roninson IB. Induction of multidrug resistance in human cells by transient exposure to different chemotherapeutic drugs. *J Natl Cancer Inst* 1993; **85**: 632–639.
2. Yang JM, Medina GY, Vassil DJ, Liao AD, Hait J. Treatment of multidrug resistant (MDR1) murine leukemia with P-glycoprotein substrates accelerates the course of the disease. *Biochem Biophys Res Commun* 1999; **266**: 167–173.
3. Yamauchi K, Yang M, Hayashi K, Jiang P, Yamamoto N, Tsuchiya H *et al*. Induction of cancer metastasis by cyclophosphamide pretreatment of host mice: an opposite effect of chemotherapy. *Cancer Res* 2008; **68**: 516–520.
4. Huber MA, Kraut N, Beug H. Molecular requirements for epithelial-mesenchymal transition during tumor progression. *Curr Opin Cell Biol* 2005; **17**: 1–11.
5. Thiery JP. Epithelial–mesenchymal transitions in tumour progression. *Nat Rev Cancer* 2002; **2**: 442–454.
6. Peinado H, Portillo F, Cano A. Transcriptional regulation of cadherins during development and carcinogenesis. *Int J Dev Biol* 2004; **48**: 365–375.
7. Barrallo-Gimeno A, Nieto MA. The Snail genes as inducers of cell movement and survival: implications in development and cancer. *Development* 2005; **132**: 3151–3161.
8. Moody SE, Perez D, Pan TC, Sarkisian CJ, Portocarrero CP, Sterner CJ *et al*. The transcriptional repressor Snail promotes mammary tumor recurrence. *Cancer Cell* 2005; **8**: 197–199.
9. Yang J, Mani SA, Weinberg RA. Exploring a new Twist on tumor metastasis. *Cancer Res* 2006; **66**: 4549–4552.
10. Mironchik Y, Winnard Jr PT, Vesuna F, Kato Y, Wildes F, Pathak AP *et al*. Twist overexpression induces *in vivo* angiogenesis and correlates with chromosomal instability in breast cancer. *Cancer Res* 2005; **65**: 10801–10809.
11. Hiscox S, Jiang WG, Obermeier K, Taylor K, Morgan L, Burmi R *et al*. Tamoxifen resistance in MCF7 cells promotes EMT-like behaviour and involves modulation of beta-catenin phosphorylation. *Int J Cancer* 2006; **118**: 290–301.
12. Kajiyama H, Shibata K, Terauchi M, Yamashita M, Ino K, Nawa A *et al*. Chemoresistance to paclitaxel induces epithelial-mesenchymal transition and enhances metastatic potential for epithelial ovarian carcinoma cells. *Int J Oncol* 2007; **31**: 277–283.
13. Li QQ, Xu JD, Wang WJ, Cao XX, Chen Q, Tang F *et al*. Twist-mediated adriamycin-induced epithelial-mesenchymal transition relates to multidrug resistance and invasive potential in breast cancer cells. *Clin Cancer Res* 2009; **15**: 2657–2665.
14. Bartel DP. MicroRNAs: genomics, biogenesis, mechanism, and function. *Cell* 2004; **116**: 281–297.
15. He L, Thomson JM, Hemann MT, Hernando-Monge E, Mu D, Goodson S *et al*. A microRNA polycistron as a potential human oncogene. *Nature* 2005; **435**: 828–833.
16. Voorhoeve PM, le Sage C, Schrier M, Gillis AJ, Stoop H, Nagel R *et al*. A genetic screen implicates miRNA-372 and miRNA-373 as oncogenes in testicular germ cell tumors. *Cell* 2006; **124**: 1169–1181.
17. Calin GA, Dumitru CD, Shimizu M, Bichi R, Zupo S, Noch E *et al*. Frequent deletions and down-regulation of microRNA genes miR-15 and miR-16 at 13q14 in chronic lymphocytic leukemia. *Proc Natl Acad Sci* 2002; **99**: 15524–15529.
18. Takamizawa J, Konishi H, Yanagisawa K, Tomida S, Osada H, Endoh H *et al*. Reduced expression of the let-7 microRNAs in human lung cancers in association with shortened postoperative survival. *Cancer Res* 2004; **64**: 3753–3756.
19. Johnson SM, Grosshans H, Shingara J, Byrom M, Jarvis R, Cheng A *et al*. RAS is regulated by the let-7 microRNA family. *Cell* 2005; **120**: 635–647.
20. Akao Y, Nakagawa Y, Naoe T. let-7 microRNA functions as a potential growth suppressor in human colon cancer cells. *Biol Pharm Bull* 2006; **29**: 903–906.
21. Yanaihara N, Caplen N, Bowman E, Seike M, Kumamoto K, Yi M *et al*. Unique microRNA molecular profiles in lung cancer diagnosis and prognosis. *Cancer Cell* 2006; **9**: 189–198.
22. Zavadil J, Narasimhan M, Blumenberg M, Schneider RJ. Transforming growth factor-beta and microRNA: mRNA regulatory networks in epithelial plasticity. *Cells Tissues Organs* 2007; **185**: 157–161.
23. Burk U, Schubert J, Wellner U, Schmalhofer O, Vincan E, Spaderna S *et al*. A reciprocal repression between ZEB1 and members of the miR-200 family promotes EMT and invasion in cancer cells. *EMBO Rep* 2008; **9**: 582–589.
24. Gregory PA, Bert AG, Paterson EL, Barry SC, Tsykin A, Farshid G *et al*. The miR-200 family and miR-205 regulate epithelial to mesenchymal transition by targeting ZEB1 and SIP1. *Nat Cell Biol* 2008; **10**: 593–601.
25. Korpala M, Lee ES, Hu G, Kang Y. The miR-200 family inhibits epithelial-mesenchymal transition and cancer cell migration by direct targeting of E-cadherin transcriptional repressors ZEB1 and ZEB2. *J Biol Chem* 2008; **283**: 14910–14914.
26. Park SM, Gaur AB, Lengyel E, Peter ME. The miR-200 family determines the epithelial phenotype of cancer cells by targeting the E-cadherin repressors ZEB1 and ZEB2. *Genes Dev* 2008; **22**: 894–907.
27. Bracken CP, Gregory PA, Kolesnikoff N, Bert AG, Wang J, Shannon MF *et al*. A double-negative feedback loop between ZEB1-SIP1 and the microRNA-200 family regulates epithelial-mesenchymal transition. *Cancer Res* 2008; **68**: 7846–7854.
28. Christoffersen NR, Silahatoglu A, Orom UA, Kauppinen S, Lund AH. miR-200b mediates post-transcriptional repression of ZFH1B. *RNA* 2007; **13**: 1172–1178.
29. Han HJ, Russo J, Kohwi Y, Kohwi-Shigematsu T. SATB1 reprograms gene expression to promote breast tumour growth and metastasis. *Nature* 2008; **452**: 187–193.
30. Mani SA, Guo W, Liao MJ, Eaton EN, Ayyanan A, Zhou AY *et al*. The epithelial-mesenchymal transition generates cells with properties of stem cells. *Cell* 2008; **133**: 704–715.
31. Davis BN, Hilyard AC, Lagna G, Hata A. SMAD proteins control DROSHA-mediated microRNA maturation. *Nature* 2008; **454**: 56–61.
32. Funatomi H, Itakura J, Ishiwata T, Pastan I, Thompson SA, Johnson GR *et al*. Amphiregulin antisense oligonucleotide inhibits the growth of T3M4 human pancreatic cancer cells and sensitizes the cells to EGF receptor-targeted therapy. *Int J Cancer* 1997; **72**: 512–517.
33. Castillo J, Erroba E, Perugorria MJ, Santamaria M, Lee DC, Prieto J *et al*. Amphiregulin contributes to the transformed phenotype of human hepatocellular carcinoma cells. *Cancer Res* 2008; **68**: 6129–6138.
34. Streicher KL, Willmarth NE, Garcia J, Boerner JL, Dewey TG, Ethier SP. Activation of a nuclear factor kappaB/interleukin-1 positive feedback loop by amphiregulin in human breast cancer cells. *Mol Cancer Res* 2007; **5**: 847–861.
35. Streicher KL, Willmarth NE, Garcia J, Boerner JL, Dewey TG, Ethier SP. Autocrine action of amphiregulin in a colon carcinoma cell line and immunocytochemical localization of amphiregulin in human colon. *J Cell Biol* 1992; **118**: 741–751.
36. Thomson S, Buck E, Petti F, Griffin G, Brown E, Ramnarine N *et al*. Epithelial to mesenchymal transition is a determinant of sensitivity of non-small-cell lung carcinoma cell lines and xenografts to epidermal growth factor receptor inhibition. *Cancer Res* 2005; **65**: 9455–9462.
37. Yauch RL, Januario T, Eberhard DA, Cavet G, Zhu W, Fu L *et al*. Epithelial versus mesenchymal phenotype determines *in vitro* sensitivity and predicts clinical activity of erlotinib in lung cancer patients. *Clin Cancer Res* 2005; **11**: 8686–8698.
38. Del Castillo G, Murillo MM, Alvarez-Barrientos A, Bertran E, Fernández M, Sánchez A *et al*. Autocrine production of TGF-beta confers resistance to apoptosis after an epithelial-mesenchymal transition process in hepatocytes: Role of EGF receptor ligands. *Exp Cell Res* 2006; **312**: 2860–2871.
39. Huber MA, Azoitei N, Baumann B, Grünert S, Sommer A, Pehamberger H *et al*. NF-kappaB is essential for epithelial-mesenchymal transition and metastasis in a model of breast cancer progression. *J Clin Invest* 2004; **114**: 569–581.
40. Kim I, Moon SO, Kim SH, Kim HJ, Koh YS, Koh GY. Vascular endothelial growth factor expression of intercellular adhesion molecule 1 (ICAM-1), vascular cell adhesion molecule 1 (VCAM-1), and E-selectin through nuclear factor-kappa B activation in endothelial cells. *Biol Chem* 2001; **276**: 7614–7620.

Supplementary Information accompanies the paper on Cell Death and Differentiation website (<http://www.nature.com/cdd>)